The Design of Polyelectrolyte Multilayers Using Galactosylated Chitosan

Hale Çiğdem Arca

Thesis submitted to the faculty of the Virginia Polytechnic Institute and State University in partial fulfillment of the requirements for the degree of

Master of Science
In
Macromolecular Science and Engineering

Padmavathy Rajagopalan, Chair
Kevin J. Edgar
Richey M. Davis

April 26, 2012
Blacksburg, VA

Keywords: Polyelectrolyte multilayers, Galactose, Chitosan, ASGP-R, Liver models

The Design of Polyelectrolyte Multilayers Using Galactosylated Chitosan

Hale Çiğdem Arca

ABSTRACT

A major challenge in hepatic tissue engineering is that liver cells rapidly lose their phenotype in *in vitro* cell culture systems. For this reason, it is necessary to design biomaterials that can support and enhance hepatic functions. Hepatocytes have a surface protein, called the asialoglycoprotein receptor (ASGP-R), which interacts with galactose via a specific receptor-ligand interaction. Polyelectrolyte multilayers (PEMs) were prepared by the layer by layer method, which is based on electrostatic attractions between oppositely charged polyelectrolytes (PEs). Anionic (hyaluronic acid) and cationic (chitosan and galactosylated chitosan) PEs were used in the fabrication of detachable, free-standing PEMs. The main focus of this study is the design of PEMs comprised of 50 bilayers of PEs. PEMs that contained galactose functional groups were assembled with either 5 or 10 bilayers of galactosylated chitosan (5 - 10 % of galactosylation). Optical properties, solvent stability and surface topography of the PEMs were measured.

For my Family

Oktay, Nurcan, Özlem and Çağla ARCA

For your unconditional Love

ACKNOWLEDGEMENTS

I would like to thank my advisor Prof. Padma Rajagopalan for the opportunities and for everything that she taught me. I would also like to thank the members of my committee, for support and input, Prof. Kevin Edgar and Prof. Richey Davis.

To my lab mates, Adam Larkin and Gaurav Jain, I owe a debt of gratitude for encouragement, experimental input, and friendship.

I am grateful for a supportive family: my parents, Oktay and Nurcan Arca, and my sisters, Özlem and Çağla Arca.

I also thank the following for financial support: National Science Foundation and Institute for Critical Technology and Applied Science (ICTAS) at Virginia Tech.

Table of Contents

List of Figures

List of Tables

List of Abbreviations

ASGP-R: Asialoglycoprotein Receptor

BL: Bilayer

CS: Chitosan

EDC: 1-Ethyl-3-(3-dimethylaminopropyl) carbodiimide

GA: Glutaraldehyde

Gal-CS: Galactosylated chitosan

HA: Hyaluronic acid

LA: Lactobionic Acid

NHS: N-Hydroxysuccinimide

PE: Polyelectrolyte

PEMs: Polyelectrolyte Multilayers

Chapter 1: Introduction and Background

1.1 Introduction to Polyelectrolyte Multilayers (PEMs)

PEMs were pioneered by Decher et al. in 1990s [1, 2] and their fabrication is based on the layer by layer method of oppositely charged PEs. As a result of the alternating adsorption of anionic and cationic PEs, self-assembled multilayers can be formed. PEMs have been used in a wide range of applications such as drug delivery [3, 4], tissue engineering [5, 6], anti-viral coatings [7, 8] and microelectronics [9].

1.1.1 Layer by Layer Method and Parameters Effecting Properties of PEMs

PEMs can be prepared either by dipping or spraying methods. In the dipping method, substrates are immersed into PE solutions and after the deposition of a PE, PEMs are dipped into washing solutions. The PEMs can be coated either on 2D surfaces [10, 11] or on 3D structures such as fibers [12, 13], microparticles or wafers [14]. In the spraying method, PEMs are prepared by spraying PE solutions onto substrates and rinsing thereafter. This accelerates the assembly time of PEMs drastically (500 times) and such multilayers are much thinner than those prepared by the dipping technique (about 70-75% less) [15].

When a solid substrate is immersed into a negatively charged PE (Polymer A) solution, a monolayer of Polymer A is deposited on the substrate and the surface becomes negatively charged. After rinsing in water, the substrate is then immersed into the positively charged PE solution (Polymer B) and a thin monolayer of Polymer B is deposited. It usually takes a couple of cycles of deposition before the surface is completely covered by the PEs [16, 17]. By repeating these steps in an alternating manner, a self-assembled multilayer is obtained which

contains both PEs [2]. Polymer concentration, molecular weight, deposition time and ionic strength [18] have influence on the thickness of PEMs [19]. Since the assembly depends on electrostatic interactions, the PEMs can be also modified by varying the pH [20], the number of bilayers [17] and the first (anchoring) layer of the multi-layer assembly [21]. Apart from these parameters, properties of PEMs can be changed by post-modification such as cross-linking [10] or addition of functional groups [22]. The differences in the fabrication of PEMs and post-modification methods will change its properties such as swelling, thickness, stiffness or optical properties.

1.1.1.1 The Effect of Salt Concentration

The adsorption of the oppositely charged PEs is an ion exchange phenomenon. The surface charge of PEs can be compensated by salt ions. At low salt concentration, PEs are very efficient in assembling on the charged substrate surface but as the salt concentration increases, it prevents the charged polymer chains from being attached to the substrate. If the salt concentration is equal to the critical salt ion concentration, the salt ions will prevent the polymer assembly on the substrate [19, 23-25].

1.1.1.2 pH Effect

The dissociation of functional groups in a PE is a property dependent on the pH of the solution. If the pH of the solution is close to the pKa value, the charge density of polymer chains decreases and this leads to the assembly of the polymer on the substrate as a thick layer and a loopy conformation [25]. This loopy conformation is not ionically cross-linked and therefore more susceptible to swelling which increases the permeability of the PEMs [26]. When there is a

difference in pH and pKa, the charge of the polymer chains decreases and this leads to the adsorption of thin rigid films [25].

1.1.1.3 The Effect of PE Structure and Dissociation Constant

The variation in the structure of the polymer can lead to different conformation of the polymer chains and thus change the property of PEMs. It is known that λ-carrageenan has the random coil conformation and ι-carrageenan has helical conformation [27]. Schoeler et al published that the film stiffness of PEMs assembled with ι-carrageenan is three times more than PEMs with λ-carrageenan [28].

The dissociation constants of PEs can influence the film thickness. Assembly of strong PEs will lead to a linear increase in the film thickness as a function of the number of bilayers [29] due to the high charge density along the backbone of the polymer, such as poly(styrene sulfonate)/poly(allylamine hydrochloride) [30] and poly(styrene sulfonate)/ poly(diallyldimethylammonium) PEMs [31].

On the other hand, the thickness of weak PEs increases exponentially with the number of bilayers, such as hyaluronic acid (HA)/poly(L-lysine) (PLL) [32, 33] and HA/chitosan (CS) PEMs [34]. This exponential increase depends on the diffusion of the polymer chains in and out of the assembled PEMs during each PE deposition step. Picart et al, demonstrated the exponential increase in film thickness in HA/PLL PEMs [32].

1.2 Introduction to Liver

1.2.1 Liver Organization and Function

The liver is divided into lobules and each lobule consists of plates of hepatocytes lined by sinusoidal capillaries. The blood supply brings many different types of endobiotics (hormones, proteins, and signaling molecules), xenobiotics (drugs, ethanol) as well as nutrients and oxygen to the liver. The liver is responsible for the detoxification of harmful substances, metabolism of amino acids, carbohydrates and lipids, and fat soluble vitamins such as vitamin A [35] and vitamin D [36], synthesis of plasma proteins such as albumin, globulin, fibrinogen, prothrombin, and antithrombin and, production of bile acids to aid fat digestion and absorption [37]. In addition, the liver takes part in the immune response in order to defend the body against pathogens such as bacteria [38]. It also converts hydrophobic substances into water soluble materials via enzymes in the endoplasmic reticulum to prevent an accumulation of lipid-soluble exogenous and endogenous compounds that are subsequently be excreted by the kidney [39]. The liver also takes part in the destruction of erythrocytes [40].

Sinusoidal cells constitute 33 % of the liver cells, which are endothelial cells (around 70% of the sinusoidal cells), Kupffer cells (liver macrophages, around 20%), fat-storing cells (stellate cells or Ito cells, around 10%) and pit cells (natural killer cells, < 1 %). Hepatocytes comprise the remaining cells [41].

1.2.2 Hepatocyte Membrane Protein: Asialoglycoprotein Receptor

ASGP-R is a calcium ion dependent [42] membrane protein, which is specific to mammalian hepatocytes. Ashwell and Morell first reported in the 1960s that glycoproteins with terminal

galactose or N-acetylgalactosamine residues are removed from the circulation *in vivo* [43]. The study was extended with the identification of liver plasma membranes as the primary binding site of asialoglycoproteins and this interaction was also shown in *in vitro* studies [44]. Pricer and Ashwell specified that the ASGP-R binding to the glycoprotein required the removal of sialic acid residues and the presence of a substituent on the plasma protein [44].

ASGP-R plays a role in the endocytosis via the clathrin coated pit pathway and degradation of a variety of desialylated glycoproteins and neoglycoproteins [45, 46]. ASGP-R binds and internalizes these asialoglycoprotein ligands via endocytic vesicles. After that, ligands are delivered to lysosomes for degradation and the receptors are recycled to the cell surface [47]. The receptors are available on the sinusoidal plasma membranes of the rat hepatocytes but not on the bile canalicular membrane [47, 48]. Hepatocytes isolated with sub-cellular fractionation of rat liver or detergent solubilization methods have about 90% of the receptors not on the cell surface but rather in Golgi, microsomal, and lysosomal membrane fractions and in segments of the endoplasmic reticulum, if asialoglycoproteins are available [49, 50]. The average number of receptors present on a cell (surface and interior) is approximately $4.5\ 10^5$ [51].

1.3 Chitosan

CS is a deacetylated derivative of chitin and a binary heteropolysaccharide which consists of (1-4)-linked 2-acetamide-2-deoxy-β-D-glucopyranose and 2-amino-2-deoxy-β-D-glucopyranose residues [52] (**Figure 1.1**).

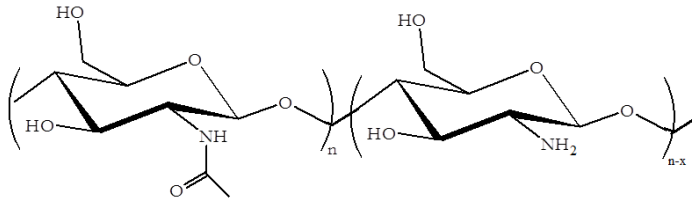

Figure 1.1 Structure of CS

Physicochemical properties of CS can change according to its molecular weight and extent of deacetylation. The degree of acetylation represents the mole fraction of acetylated units in the polymer chain, the proportion of N-acetyl-D-glucosamine units with respect to the total number of monomers. Generally, CS has a degree of deacetylation 50 % or above [53].

CS can degrade *in vivo* via enzymatic hydrolysis by lysozyme. It is insoluble in water and organic solvents but becomes soluble in dilute acidic solutions (pH < 6.0 - 6.5), when its primary amino groups become protonated. This renders the molecule positively charged [54, 55] and makes it a cationic PE. It precipitates in alkaline solution or forms gels with anionic PE at lower pH [56, 57]. Due to the cationic nature of CS, it can interact with anionic glycosaminoglycans, proteoglycans and other negatively charged molecules [55] such as HA [58]. It has the ability to form films [10, 59, 60] and can be used as a sponge, gel or microcapsules [58]. CS is a promising polymer for tissue engineering due to its favorable properties. These include CS being nontoxic, non-allergenic, antimicrobial, biocompatible and biodegradable [61-63]. It has structural similarity to glycosaminoglycans which are a major component of the extracellular matrix (ECM) [63], and stimulates attachment, proliferation and viability of cells including stem cells, and also the retention of cell morphology [55]. It is compatible with hepatocytes [64, 65]. Moreover, amino and hydroxyl groups of CS can be chemically modified with a variety of ligands.

1.4 Hyaluronic Acid

HA is a linear polysaccharide and an alternating copolymer of glucuronic acid and *N*-acetylglucosamine. It is a natural material with a high molecular weight (10^5 to 10^7 Dalton) and lacks immunogenicity. Its chemical composition (**Figure 1.2**) is identical for both humans and animals thus it can be isolated from rooster combs or streptococci cultures [66].

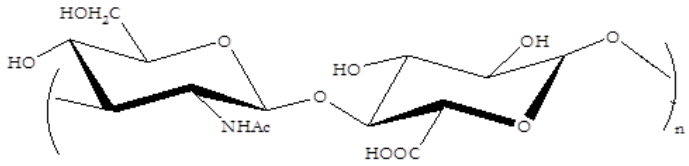

Figure 1.2 Structure of HA

HA is a component of the ECM in most tissues [67]. It is the only sulfate group free glycosaminoglycan and does not have a proteoglycan primer. Therefore it cannot form a proteoglycan. Its viscosity depends on the concentration, and this polysaccharide can form very viscous solutions but not a gel [68]. HA is a weak PE with good biocompatibility, nontoxicity, and biodegradability [69]. Due to these properties, it has been used in tissue engineering [70] and drug delivery [71].

Chapter 2. Synthesis of Galactosylated Chitosan and Accompanying Characterization

2.1 Introduction

Galactose is a 6C sugar that is a C-4 epimer of glucose. The structure of galactose is presented in **Figure 2.1.**

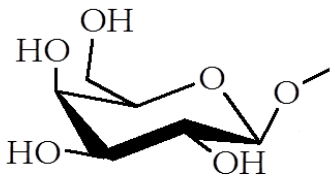

Figure 2.1 Structure of β-D-Galactopyranose

The free amino groups of CS are easily modified with the introduction of galactose group by carbodiimide chemistry. This chemical modification increases its bioactivity.

1-Ethyl-3-(3-dimethylaminopropyl) carbodiimide (EDC) is a favorable carbodiimide for use in conjugating biomaterials since it is water soluble and can be directly added to the reaction medium without the use of an organic solvent. The pH of the reaction medium typically ranges between 6.0-7.0 [72]. N-hydroxyl succinimide (NHS) esters are typically added to EDC reactions.

The introduction of galactose into CS results in galactosylated chitosan (Gal-CS) which can be further used as a scaffold biomaterial for hepatic tissue engineering. This has been successfully used to prepare cell culture substrates [73]. Adhesion of hepatocytes on galactosylated substrates are mediated by the galactose-specific interactions between ASGP-R of the hepatocytes and galactose residues present on the surface of the substrates [74, 75].

2.2 Materials and Methods

2.2.1 Materials

Medium molecular weight CS (≈350 kDa), N-Hydroxysuccinimide (NHS) and deuterium oxide (D_2O) were obtained from Sigma-Aldrich (St. Louis, MO). 1-Ethyl-3-(3-dimethylaminopropyl) carbodiimide (EDC), lactobionic acid (LA), trifluoroacetic acid-d (CF_3COOD), acetic acid (CH_3COOH) and acetone were received from Fischer Scientific (Pittsburgh, PA). Dialysis membranes were obtained from Spectrum Laboratories (Rancho Dominguez, CA) with a MWCO 3500.

2.2.2 Calculation of the Extent of Acetylation in CS

Deacetylation degree of CS was calculated by ^{1}H-NMR of 10 samples from the same batch of CS. 0.005 g Gal-CS was dissolved in 1 ml D_2O and 10 µl CF_3COOD solution. The solution was mixed for 3 hours and then transferred to NMR tubes for analysis. ^{1}H-NMR spectra were measured using INOVA 400 spectrometer, (VARIAN, Palo Alto, CA). The proportion of N-acetyl-D-glucosamine units with respect to the total number of monomers was calculated by using the integral intensity proportions of -CH_3 peak of acetyl group of CS, and the sum of integral intensities, H_2, H_3, H_4, H_5, H_6, and H_6' protons.

2.2.3 Synthesis and Purification of Gal-CS

Galactose-containing LA was covalently coupled with CS using carbodiimide chemistry. Briefly, 0.44 g CS was added to 30 ml deionized (DI) water with 200 µl of acetic acid. This solution was stirred until the polymer was dissolved and a clear solution was obtained. In another beaker, 0.44 g LA, 0.035 g NHS and 0.12 g EDC were dissolved in 2 ml DI water. Then

this solution was carefully added to the CS solution. After 15 min, the pH was measured. The reaction was stirred at room temperature for 3 days.

Table 2.1 Syntheses for Different Extents of Galactosylation

Percentage of galactosylation	CS (g)	LA (g)	NHS (g)	EDC (g)	pH
5 %	0.44	0.44	0.035	0.12	5.7-6.0
10 %	0.44	0.88	0.07	0.24	5.7-6.0
15 %	0.44	1.25	0.10	0.36	5.7-6.0

After the synthesis, the polymer was purified by dialysis for 4 days against distilled water, precipitated with acetone and then dried at room temperature overnight.

2.2.4 ^{1}H-NMR Measurements

0.005 g Gal-CS was dissolved in 1 ml D_2O and 10 µl CF_3COOD. The solution was mixed for 3 hours and then transferred to NMR tubes for analysis. ^{1}H-NMR spectra were measured on an INOVA 400 spectrometer, (VARIAN, Palo Alto, CA).

2.2.5 FTIR Sample Preparation and Measurement

After precipitation with acetone, the polymer was placed on a p-tetrafluoroethylene (PTFE) substrate and dried at room temperature. FTIR spectra were obtained on a M series FTIR spectrometer (MIDAC Corporation, Westfield, MA).

2.3 Results

The method Hirai et al [76] developed was used to calculate the degree of deacetylation of CS by using the integral intensity proportions of acetyl groups and the sum of integral intensities, H_2, H_3, H_4, H_5, H_6, and H_6' protons (**Figure 2.2**) in a ^{1}H-NMR spectrum.

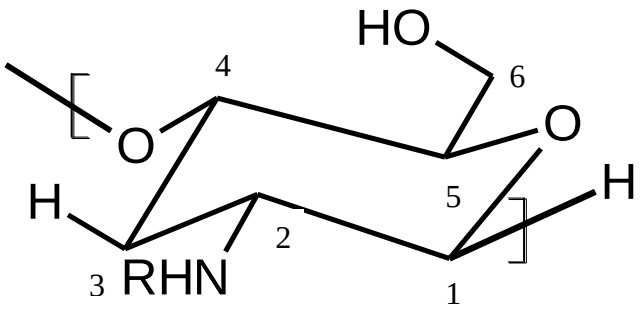

Figure 2.2 CS Structure to Show the Proton Numbers

The formula used to calculate the degree of acetylation of CS:

$$\text{Acetylation degree} = \frac{\frac{1}{3}\left(I_{CH_3}\right)}{\frac{1}{6}\left(I_{H_2-H_6}\right)} \text{ x } 100$$

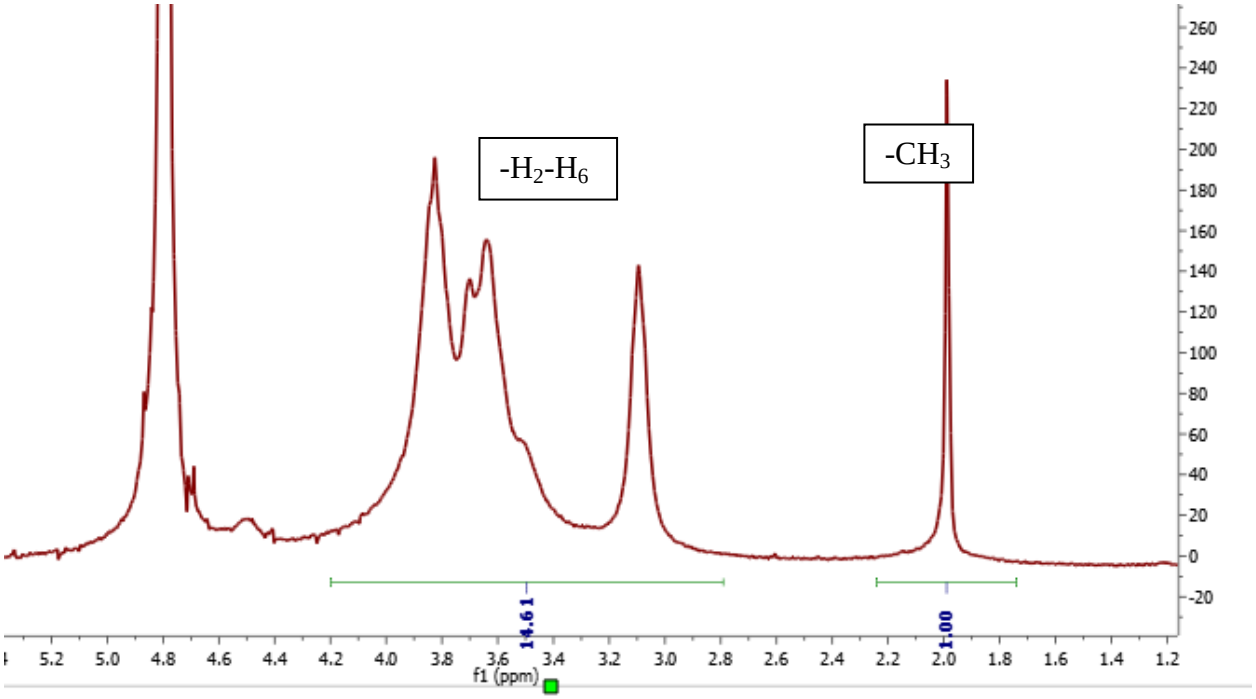

Figure 2.3 400 MHz ^{1}H NMR spectrum of CS in CF_3COOD/D_2O

In **Figure 2.3**, the intensity of the $-CH_3$ peak is 1.00 and the intensity of the H_2-H_6 protons are 14.61. The deacetylation of this sample was calculated to be 86.31 %.

Acetylation % = [(1/3 (1.00) / 1/6 (14.61)] x 100 = 13.69 %

These calculations were performed for 10 different samples and the data are shown in **Table 2.2**.

Table 2.2 Summary of the Extent of CS Acetylation

Number of CS Samples	Acetylation Percentage of CS
10	14.16 % ± 5.54

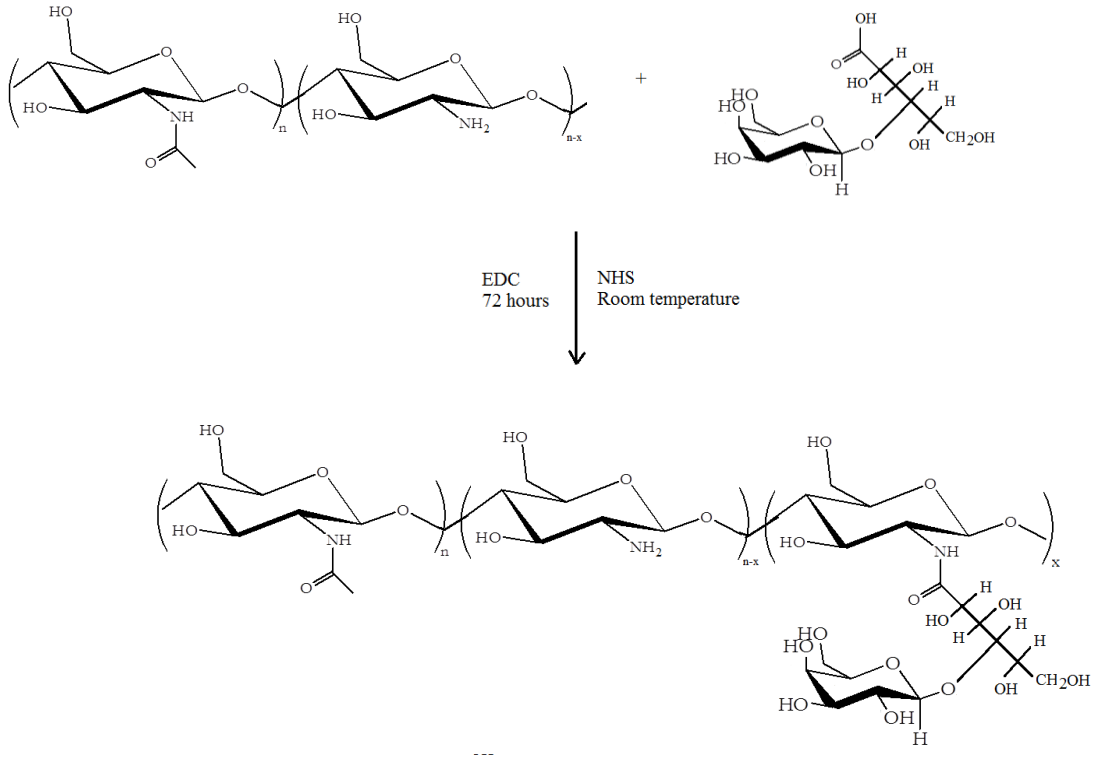

Figure 2.4 Synthesis Scheme of Gal-CS

The synthesis scheme of Gal-CS is shown on **Figure 2.4**. Gal-CS was prepared with EDC, NHS and LA. EDC carbodiimide chemistry has already been used to prepare Gal-CS [77, 78]. EDC is a zero length cross-linker and participates in carboxyl to amine group conjugation. Based upon to this mechanism, Gal-CS was prepared at a pH 5.7-6.0 and the ligand addition was supported by ^{1}H-NMR and FTIR measurements.

The introduction of LA to CS is an established method for preparing Gal-CS [75, 79-81]. In all of these studies, *N*,*N*,*N*',*N*'-tetramethylethylenediamine (TEMED)/HCl solution was first introduced to the reaction medium, then stirred for 72 h, purified, and finally freeze dried in order to obtain a dry polymer for further experiments. It was observed that TEMED did not contribute to the galactosylation reaction; by contrast, it decreases the galactosylation percentage of the synthesis as shown in **Table 2.3**. Therefore, subsequent syntheses of gal-CS were performed without the addition of TEMED.

Table 2.3 The Effect of TEMED on Galactosylation

CS (mol)	**LA (mol)**	**NHS (mol)**	**EDC (mol)**	**TEMED (ml)**	**Time (days)**	**Extent of Galactosylation (%)**
$6.46\ 10^{-3}$	$6.42\ 10^{-3}$	$1.22\ 10^{-3}$	$3.86\ 10^{-3}$	0.2-0.3	6	≈10 [73]
$1.3\ 10^{-3}$	$5.53\ 10^{-4}$	$2.48\ 10^{-4}$	$7.74\ 10^{-4}$	0	3	≈15

In addition not contributing to the galactosylation synthesis, TEMED causes many other problems. Although TEMED is added at very small amounts, it cannot be removed in the purification process by dialysis alone requiring another method to remove the organic solvent. By not adding TEMED, it is possible to precipitate Gal-CS with acetone as shown in **Figure 2.5**, and the precipitation takes less than 10 min and dries overnight.

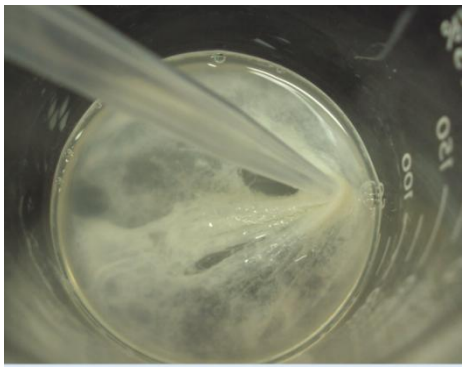

Figure 2.5 Precipitation of Gal-CS by Acetone to Show rapid Polymer Precipitation

Gal-CS is characterized by ^{1}H-NMR. The peak at 4.1 ppm is a characteristic peak of LA shown in **Figure 2.6 (A)**. It does not overlap with CS peaks, which are observed at 2.0 ppm and 2.9 to 4.0 ppm. The peaks of LA at 3.4 to 4.0 ppm overlap with the CS backbone peaks. Therefore it is very hard to distinguish LA peaks from CS peaks in this region. Observation of the 4.1 peak in **Figure 2.6 (B and C)** indicates the conjugation of Gal to CS. The extent of galactosylation was calculated according to the intensity ratios of the specific LA peak at 4.1 and the $-CH_3$ peak of acetyl group of CS at 2.0 ppm. Based upon our previous calculation for deacetylation and, the number and intensity of the $-CH_3$ peak the extent of galactosylation was calculated.

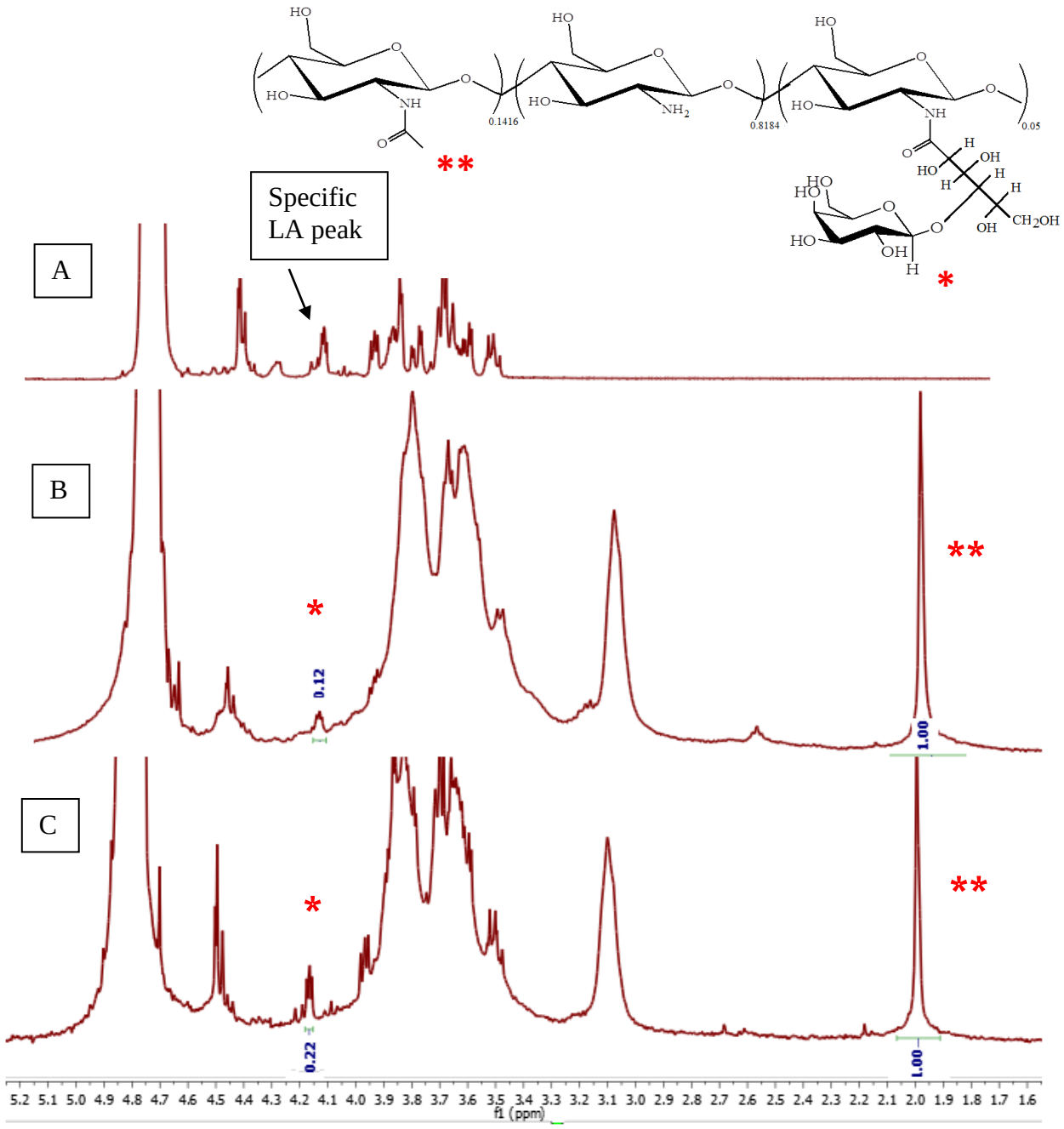

Figure 2.6 400 MHz ^{1}H NMR Spectrum of LA (A), 5.09 % Gal-CS (B) and 9.34 % Gal-CS (C) in CF_3COOD/D_2O

1.00/3 = 0.333 represents 1 hydrogen of the acetyl peak and this group is present on 14.16 % of the monomers in the chain.

0.3333 → 14.16 %

0.12 → x

---

x= 5.09 % galactose group

The extent of galactosylation of this polymer is 5.09 % according to the ^{1}H-NMR spectra. Based on the above calculation method, 5 %, 10 % and 15 % Gal-CS batches were prepared.

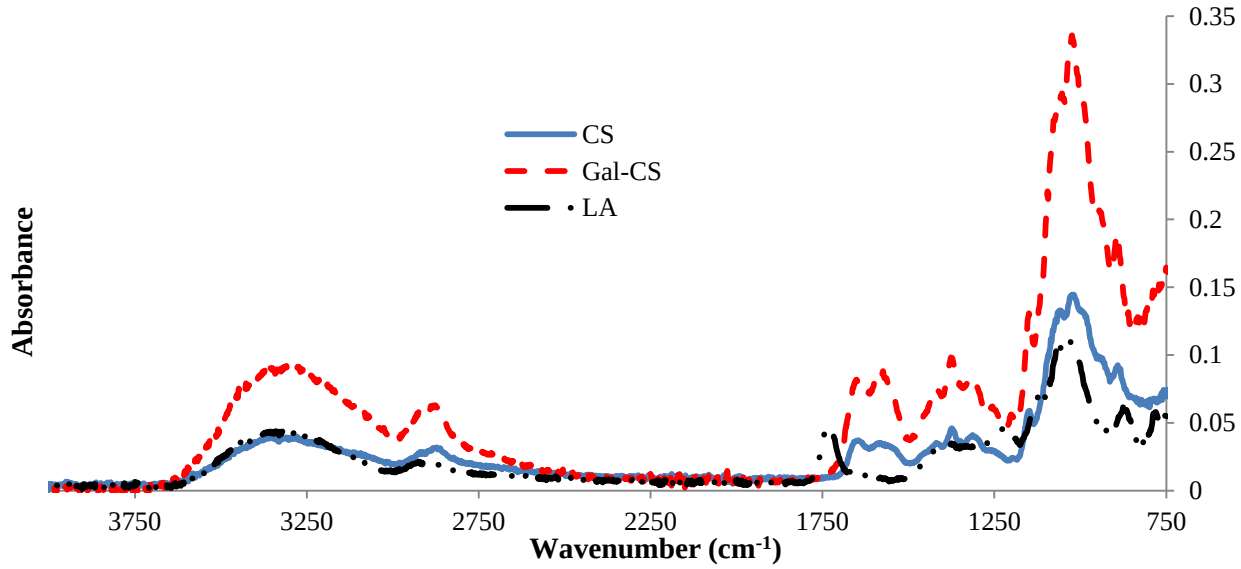

Figure 2.7 FTIR Spectra in the 750 - 4000 cm^{-1} Range for Gal-CS, CS and LA

Figure 2.7 shows the FTIR spectra of CS, Gal-CS and LA. FTIR measurements further indicated the chemical attachment of LA to the primary amine group of CS. A carbonyl group stretching peak of LA is observed at 1712 cm^{-1} but not on the spectrum of Gal-CS. This data shows that the carboxylic acid peak is not present after the galactosylation reaction.

The normalized absorbance values of Gal-CS peaks were compared to the CS peaks and the normalization was based on the –CH stretching peak at 2850 cm^{-1}. CS has characteristic amide peaks at 1683 cm^{-1} and 1538 cm^{-1}, shown on **Figure 2.7**. In the spectra of Gal-CS, the amide

bands I and II shift were at 1623 cm^{-1} and 1558 cm^{-1}, respectively. Absorbance values of Gal-CS peaks were higher than the CS peaks. Similar trends were observed for the amide II band (N-H), amide I band (C=O), the NH and OH stretching vibrations (3200-3500 cm^{-1}).

The molecular weights for the repeat units of CS, 5 % Gal-CS and 10 % Gal-CS were calculated. According to this the repeating molecular weight was calculated:

203 x 0.1416 + 161 x 0.8684 = 166.88 g

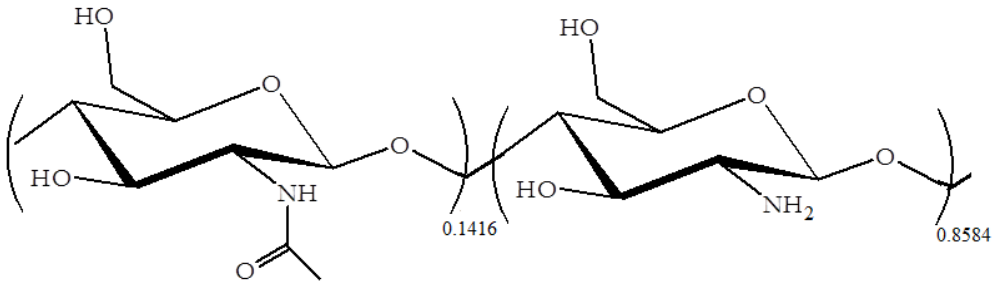

Figure 2.8 CS Repeating Unit Molecular Weight Calculation

The repeating unit molecular weight of 5 % Gal-CS is (**Figure 2.9**):

203 x 0.1416 + 161 x 0.8684 + 501 x 0.05 = 183.88 g

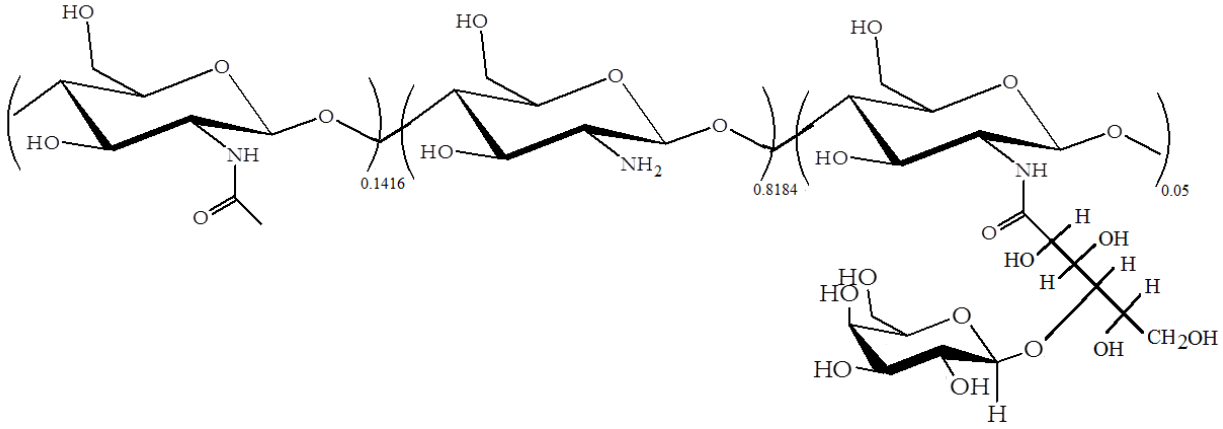

Figure 2.9 5 % Gal-CS Repeating Unit Molecular Weight Calculation

The repeating unit molecular weight of 10 % Gal-CS is (**Figure 2.10**):

203 x 0.1416 + 161 x 0.7684 + 501 x 0.10 = 200.88 g

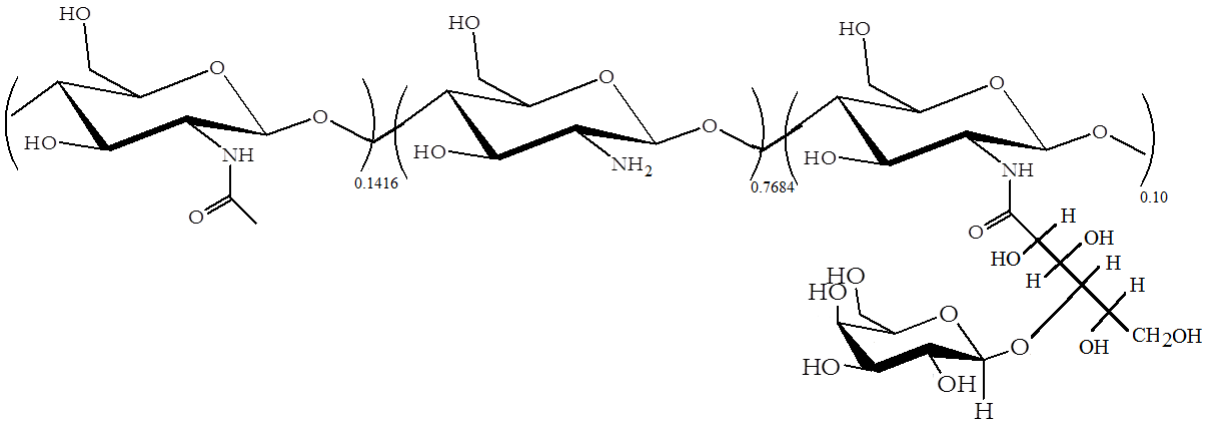

Figure 2.10 10 % Gal-CS Repeating Unit Molecular Weight Calculation

Chapter 3. Assembly of Polyelectrolyte Multilayers with Gal-CS and Accompanying Characterization

3.1 Introduction

The assembly of PEMs is based on the electrostatic attraction between opposite charged PEs. In this study, detachable and free-standing PEMs based on Gal-CS were assembled. In each PEM, up to 10 bilayers of the assembly were comprised of Gal-CS and HA and, subsequent bilayers contained CS and HA.

It was reported that the water content is very high in the polysaccharide based PEMs ranging from 70 - 90 % [82]. HA and CS are highly hydrated polymers, which interacts 20 - 30 water molecules per disaccharide via hydrogen bonds [82]. Boudou at al showed that water content of HA/CS PEMs can reach to 80 % [83]. Therefore the water content of the hydrated CS/HA and Gal-CS/HA/CS PEMs can be $\geq$ 70 %.

In this study, 50 BL detachable, free-standing Gal-CS/HA/CS PEMs were designed. 5 % and 10 % Gal-CS was used to prepare 5 or 10 BL of 50 BL PEMs. Gal-CS was assembled on one surface.

3.2 Materials and Methods

3.2.1 Materials

Chitosan (Mw $\approx$ 350 kDa) and glutaraldehyde (GA) were obtained from Sigma-Aldrich (St. Louis, MO). Hyaluronic acid (HA, Mw $\approx$ 750 kDa), and acetic acid were obtained from Fluka (St. Louis, MO). PTFE substrates were obtained from McMaster Carr Supply Company

(Aurora, OH). Phosphate buffered saline (10XPBS; 137 mM NaCl, 2.7 mM KCl, 10 mM Na_2HPO_4) was obtained from Invitrogen Life Technologies (Carlsbad, CA). All other chemicals were received from Fischer Scientific, (Pittsburgh, PA), unless noted otherwise.

3.2.2 Assembly of Detachable and Free-standing PEMs

HA was used as the anionic PE and, CS and Gal-CS were the cationic PEs in the assembly of the detachable PEMs. HA solutions were prepared with 18 MΩ cm Picopure water (hydro, Raleigh NC). CS and Gal-CS solutions were first dissolved in 1 % v/v acetic acid. The solution concentrations of CS and HA were 2 mM and 1 mM for 50 bilayer PEMs, and 10 mM and 5 mM for 15 BL PEMs respectively. The solution concentrations were calculated based upon the repeat unit molecular weight of the polymer, 166.88 g mol^{-1} for CS and 874.7 g mol^{-1} for HA. The solution concentrations of 5 % Gal-CS are 1.89 mM and 9.2 mM for the 50 bilayer and 15 bilayer solutions, respectively. The solution concentrations of 10 % Gal-CS are 1.7 mM and 8.5 mM for the 50 bilayer and 15 bilayer solutions, respectively. The molecular weights of the 5 % and 10 % Gal-CS are 183.88 g mol^{-1} and 200.88 g mol^{-1}. The solutions were filtered through a 0.45 µm polyethersulfone filters (Nalgene, Rochester NY). The pKa value of HA is about 3.0 [84] and pKa of CS is 6.5 [85].

The pH of the solutions was 4.0 for HA, 5.0 for CS and Gal-CS, and 4.5 for water in the 50 BL PEMs preparation. The PEMs were assembled on inert hydrophobic PTFE substrates by using a robotic deposition system (NanoStrata, Gainesville, FL). The PTFE substrates were cleaned by sonication in toluene for 1 hour. The hydrophobicity of the clean substrates was measured by using static water contact angle measurements (KSV Instruments, Helsinki, Finland). The

average contact angle was 111.35 ± 3.1° (averaged over 3 different samples, around 30 different measurements per sample). PEMs with different properties were prepared by varying polymer deposition time, polymer concentrations, pH of solutions and cross-linking conditions. The preparation of PEMs started with the deposition of the negative PE, HA followed by the cationic PE (CS or Gal-CS), alternately. After each deposition, the assembly was rinsed in water for 4 min. One bilayer is composed of one anionic and one cationic PE. 50 and 15 bilayer detachable PEMs were prepared with different deposition times such as 20 min, 40 min or 50 min. After that, PEMs were dried at room temperature overnight and detached from the underlying surface. PEMs that did not detach from the substrate were denoted as "un-detachable" and those with tears were noted as "cracks appeared". PEMs were cross-linked with either 4 w/v % or 8 w/v % GA. The range for the exposure time to the cross-linker was 20 sec to 40 sec for 15 BL PEMs and 1 min to 2 min for 50 BL PEMs. PEMs were washed with water for 2 days and dried at room temperature overnight. These PEMs will be named "washed PEMs" in the subsequent sections. PEMs were kept at room temperature until further use and detached prior to experimentation.

3.2.3 Aqueous Stability of PEMs

Detachable 50 BL Gal-CS/HA/CS PEMs were peeled from the substrate and weighed. After that they were placed in 1XPBS at 37°C and up to 7 days. After 7 days, PEMs were rinsed with DI water and dried at 50°C for 4 days under vacuum. The weight of the sample, before and after incubation to PBS was obtained.

3.2.4 Thickness Measurements

A profilometer (Veeco Dektak 150, Veeco Metrology, Santa Barbara, CA) was used to measure the thickness on the PEMs. 9 measurements were obtained per sample at dry conditions at a scan length of 1000 μm.

3.2.5 Optical Properties

The optical properties of PEMs were measured on a UV/vis spectraphotometer (Perkin Elmer Lambda 25, Downers Grove IL) between 400 - 900 nm. The optical transparencies of both dry and hydrated PEMs were measured.

3.2.6 Atomic Force Microscopy (AFM)

The surface topography of the detachable PEMs was measured with AFM (Veeco Multimode AFM, Santa Barbara CA). Silicon nitrite DNP tips with a spring constant of 0.12 N/m (Veeco, Santa Barbara CA) were used in contact mode at a scanning rate of 2 Hz. The data was analyzed by using Nanoscope software (Veeco, Santa Barbara CA) to determine the surface roughness of PEMs.

3.3 Results

Anionic PE (HA) and cationic PEs (Gal-CS and CS) were sequentially assembled on clean, inert and hydrophobic PTFE substrates. The detachability of PEMs was dependent on the concentration of the PE solutions, PE deposition time, total number of bilayers, galactosylation percentage and, the number of bilayers that contained Gal-CS. The ease of detachment increased as the total number bilayers, concentration of the solutions and deposition time of PE was higher.

3.3.1 Results of 50 BL PEMs

50 BL free standing detachable CS/HA PEMs were previously prepared in our group at 8 w/v % GA for 1 min and 2 min [10]. These PEMs were modified with 5 % and 10 % Gal-CS at the conditions shown in **Table 3.1**. The galactosylated polymer is assembled on the substrate side of the PEMs for each multilayer. The substrate side of the PEMs indicates the side of the PEM in contact with the PTFE substrate and the air-side denotes the side of PEMs in contact with air (**Figure 3.2**).

Table 3.1 Conditions of Washed, Detachable 50 bilayer PEMs with 20 min Deposition Time, [HA] = 1 mM, [CS] = 2 mM, [Gal-CS] = 1.8 mM

Extent of galactosylation (%)	Number of BL with Gal-CS	Cross-linking condition (w/v)	Detachable
5	5	Un-modified	Yes
5	5	1 min 4 % GA	Yes
5	5	2 min 4 % GA	Yes
5	5	1 min 8 % GA	Yes
5	5	2 min 8 % GA	Yes
5	10	Un-modified	Yes
5	10	1 min 4 % GA	Yes
5	10	2 min 4 % GA	Yes
5	10	1 min 8 % GA	Yes
5	10	2 min 8 % GA	Yes
10	5	Un-modified	Yes
10	5	1 min 4 % GA	Yes
10	5	2 min 4 % GA	Yes
10	5	1 min 8 % GA	Yes
10	5	2 min 8 % GA	Yes
10	10	Un-modified	Yes
10	10	1 min 4 % GA	Yes
10	10	2 min 4 % GA	Yes
10	10	1 min 8 % GA	No
10	10	2 min 8 % GA	No

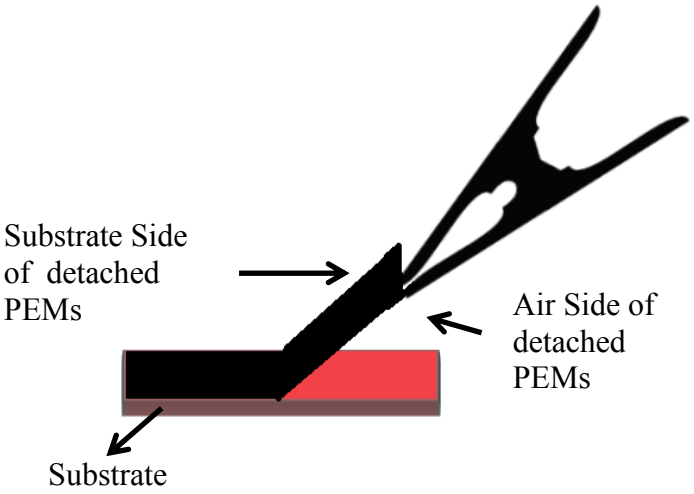

Figure 3.1 Schematic to Show the Surface and Air Side of the PEMs

5 % and 10 % Gal-CS PEMs were cross-linked with 4 w/v % and 8 w/v % GA for 1 and 2 min. GA increases the rigidity of the PEMs, however it is a known cytotoxin [86]. To be able to use the PEMs for biological application, it is necessary to remove GA by washing. In this study, methods, cross-linked PEMs were rinsed in DI water for 2 days. Four different cross-linking conditions of PEMs were tested for this study to investigate the effects of cross-linking on mechanical properties and cellular responses. These effects have not been investigated in this study and will be the focus of future investigations.

PEMs with 10 BL 10 % Gal-CS cross-linked with 8 w/v % GA were not detachable (**Table 3.1**). On the other hand, PEMs with 5 % Gal-CS and 5 BL 10 % Gal-CS/HA/CS PEMs were detachable.

Figure 3.2 shows 50 BL PEMs assembled with Gal-CS/HA/CS.

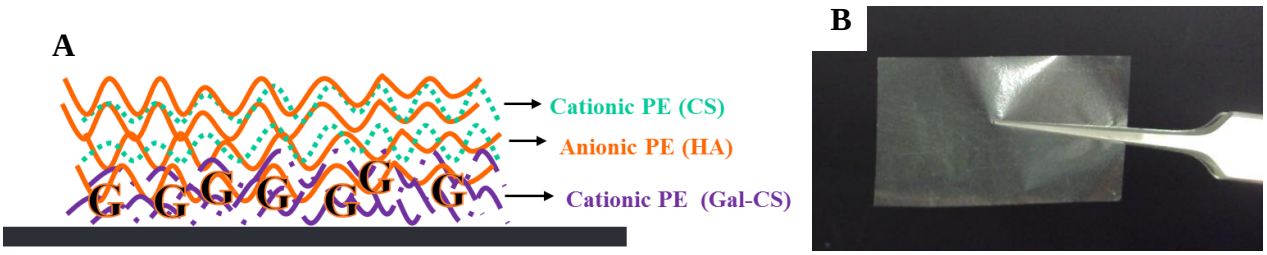

Figure 3.2 (A) Assembly of 50 BL Gal-CS/HA/CS PEMs and (B) a detached 50 BL PEMs which includes 5 BL of 5 % Gal-CS

The aqueous stability is important for biological applications. PEMs that are not cross-linked degrade within 5min when placed in 1XPBS. Cross-linked PEMs with 4 w/v % and 8 w/v % GA for 1 or 2 min were monitored over a period of 7 days. According to the results presented in **Figure 3.3**, the weight retention over a seven day period is more than 90 % in the PEMs assembled with 5 bilayers of 5 % Gal-CS/HA/CS cross-linked with 8 w/v % and 4 w/v % GA. The weight retention percentage is 82.6 ± 6.4, 94.3 ± 2.2, 96.4 ± 1.9 and 96.9 ± 2.6 for 4 w/v % GA for 1 min and 2 min and 8 % w/v GA 1 min and 2 min conditions respectively. Since the weight loss was more than 10 % in 5 % Gal-CS 5 bilayer 4 w/v % GA 1 min cross-linked condition, this PEM was not considered for further experimentation.

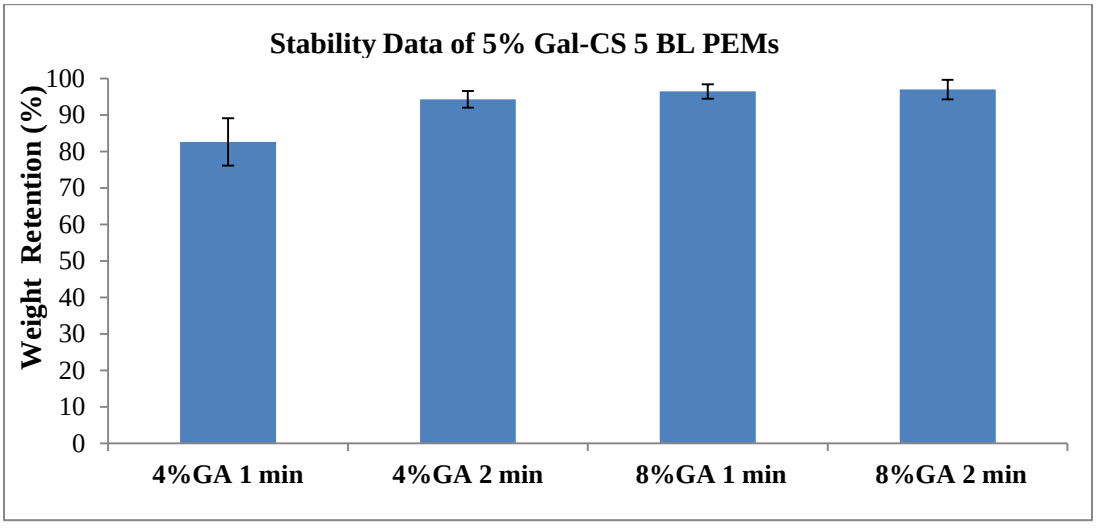

Figure 3.3 Stability Data of 50 BL 5 % Gal-CS PEMS with 20 min Deposition (n=3)

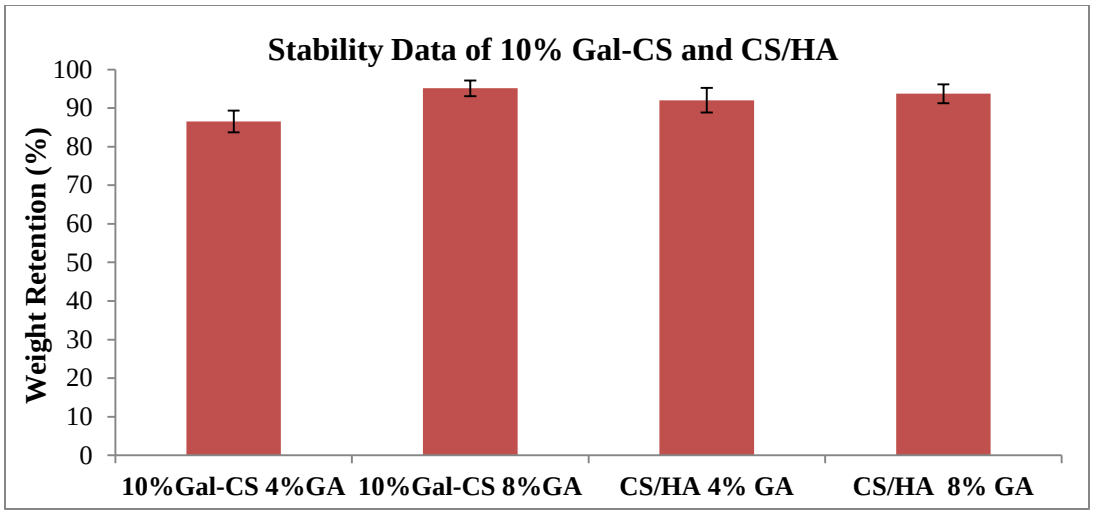

Figure 3.4 Stability Data of 50 BL 10 % Gal-CS and CS/HA PEMs with 20 min Deposition, Cross-linked for 2 min (n=3)

The stability data of 10 % Gal-CS/HA/CS and CS/HA PEMs cross-linked with 4 w/v and 8 w/v % GA for 2 min is shown in **Figure 3.4**. Briefly, weight retention percentage of the 10 % Gal-CS/HA/CS PEMs 4 w/v % and 8 w/v % GA and CS/HA 4 w/v % and 8 w/v % GA cross-linking conditions are 86.54 ± 2.81, 95.12 ± 2.1, 92.01 ± 3.1 and 93.7 ± 2.42 respectively.

The thickness of 50 BL dry PEMs, where 5 BLs were prepared with 5 % or 10 % Gal-CS were measured by profilometry. The results are shown in **Table 3.2 and Table 3.3**.

Table 3.2 Thickness of dry 5 BL 5 % Gal-CS/HA/CS PEMs, Total Number of BL 50 (n=9)

1 min 4 w/v % GA (nm)	**2 min 4 w/v % GA (nm)**	**1 min 8 w/v % GA (nm)**	**2 min 8 w/v % GA (nm)**
2329 ± 69	2702 ± 31	2585 ± 14	2804 ± 28

Table 3.3 Thickness of dry 5 BL 10 % Gal-CS/HA/CS PEMs, Total number of BL 50 (n=9)

2 min 4 w/v % GA (nm)	2 min 8 w/v % GA (nm)
2380 ± 81	2392 ± 110

UV-transmission of the PEMs was measured to determine their optical transparency. Measurements were taken in the visible light range of 400 to 900 nm. Transmission of hydrated and dry samples was measured for unmodified samples and samples at different cross-linking conditions. In the dry state, the transmission of 10 % 5 BL Gal-CS/HA/CS PEMs (unmodified or cross-linked) was between 61 – 66 % and the transmission of 10 % 10 BL Gal-CS/HA/CS PEMs (unmodified or cross-linked) was 50 – 70 %. In the hydrated state, the transmission of 10 % 5 BL Gal-CS/HA/CS PEMs (unmodified or cross-linked) was between 94 – 97 % as shown in **Figure 3.5** and **Figure 3.6** and for 10 BL PEMs the range was 93 – 98 % as shown in **Figure 3.7**. According to these data, all PEMs have transmission higher than 95 % in the hydrated state. The decrease observed at lower wavelengths in the percent transmission can be attributed to scattering (**Figure 3.5, Figure 3.6 and Figure 3.7**).

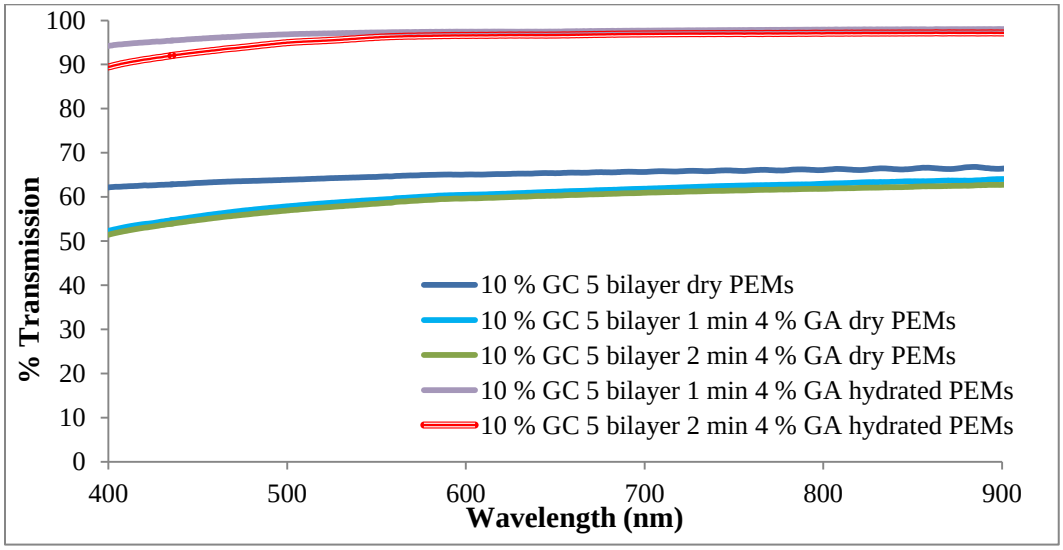

Figure 3.5 Optical Transmission in the 400 – 900 nm Range for the Dry and Hydrated 50 BL PEMs, 5 BL Prepared with 10 % Gal-CS and Cross-linked with 4 w/v % GA

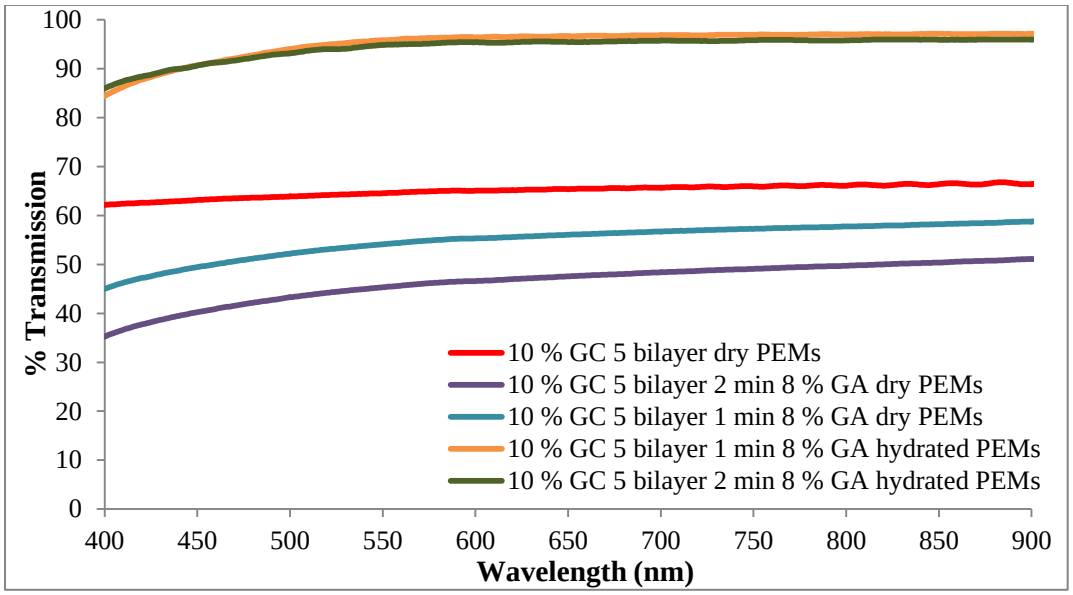

Figure 3.6 Optical Transmission in the 400 – 900 nm Range for the Dry and Hydrated 50 BL PEMs, 5 BL Prepared with 10 % Gal-CS and Cross-linked with 8 w/v % GA

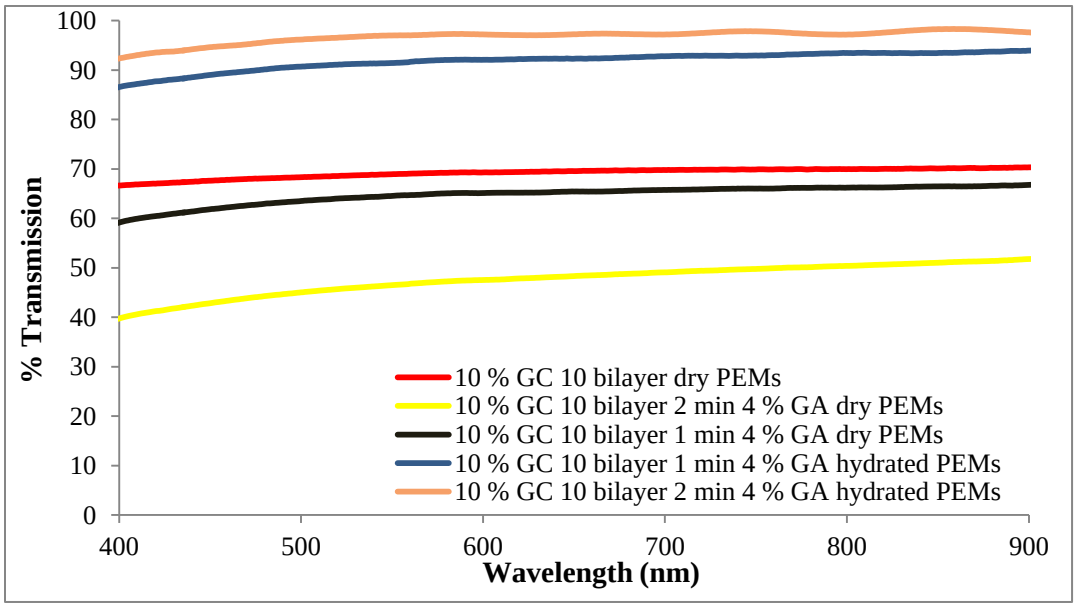

Figure 3.7 Optical Transmission in the 400 – 900 nm Range for the Dry and Hydrated 50 BL PEMs, 10 BL Prepared with 10 % Gal-CS and Cross-linked with 4 w/v % GA

The surface topographies of 5 % Gal-CS/HA/CS PEMs and CS/HA PEMs at 4 w/v % GA for 2 min and 8 % w/v GA for 2 min cross-linking conditions were measured to determine roughness.

The surface topography of the air side of the 5 % Gal-CS/HA/CS PEMs was investigated using AFM and the images are presented in **Figure 3.8**. No significant changes were observed as a result of Gal-CS (**Figure 3.9**). The substrate side roughness of 4 % and 8 % GA cross-linked 5 % Gal-CS PEMs are 1.94 ± 0.55 nm and 2.25 ± 0.09 nm, respectively. The substrate side roughness of 4 % and 8 % GA cross-linked CS PEMs are 1.66 ± 0.05 nm and 2.3 ± 0.62 nm, respectively. The air side roughness of 4 % and 8 % GA cross-linked 5 % Gal-CS PEMs are 4.04 ± 2.09 nm and 4.3 ± 1.51 nm, respectively.

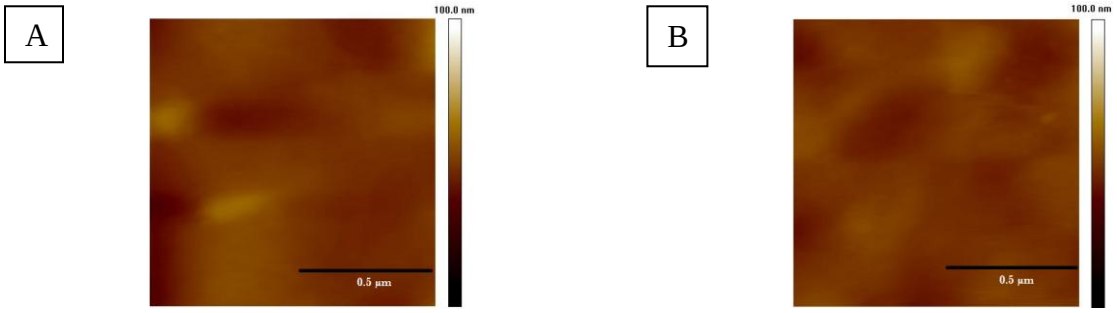

Figure 3.8 Air Side AFM Images of 50 BL 20 min Deposition PEMs 5 BL 5 % Gal-CS /HA/CS PEMs: A) Cross-linked with 8 w/v % GA for 2 min, B) Cross-linked with 4 w/v % GA for 2 min

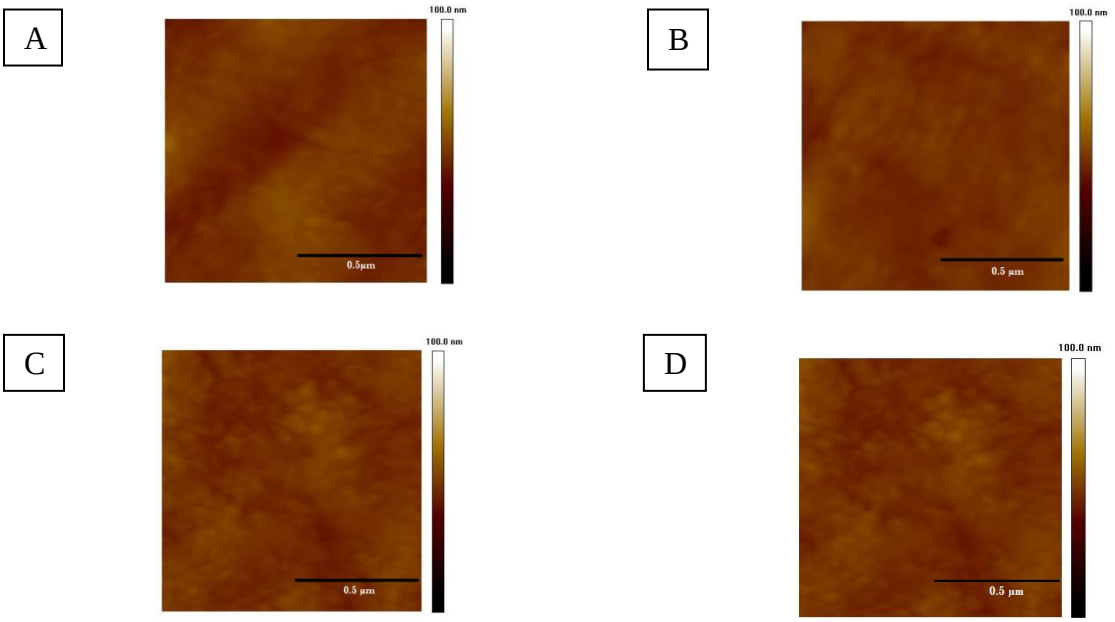

Figure 3.9 Substrate Side AFM Images of 50 BL 20 min Deposition PEMs: A) 5 BL 5 % Gal-CS/HA/CS PEMs Cross-linked with 8 w/v % GA for 2 min, B) 5 BL 5 % Gal-CS/HA/CS PEMs Cross-linked with 4 w/v % GA for 2 min C) CS/HA PEMs Cross-linked with 8 w/v % GA for 2 min D) CS/HA PEMs Cross-linked with 4 w/v % GA for 2 min

3.3.2 Results of 15 BL PEMs

15 BL free standing detachable Gal-CS/HA/CS PEMs were prepared with 8 w/v % GA 30 sec crosslinking condition. The aim of this study was to prepare thin PEMs, whose thickness will be within the range of 500 - 1000 nm under hydrated conditions. The assembly conditions of 5 % and 10 % Gal-CS PEMs are shown in **Table 3.4**. The galactosylated polymer is assembled on the substrate side of the PEMs. The optimum conditions for 15 BL 5 % and 10 % Gal-CS PEMs are obtained with 50 min deposition time, and pH of the Gal-CS, HA, water and CS solutions were 4.0, 4.0, 4.0 and 5.0 respectively. 15 BL PEMs were cross-linked with 8 w/v % GA for 30 sec. 15 BL CS/HA PEMs were also prepared at the same conditions to be compared with the Gal-CS/HA/CS PEMs and the CS/HA PEMs were robust and detachable.

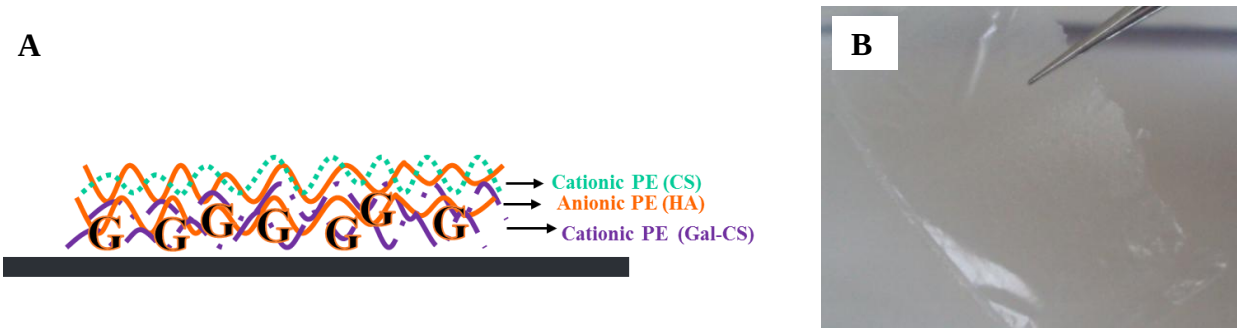

Figure 3.10 (A) Illustration of 15 BL Gal-CS/HA/CS PEMs on Substrate and (B) a picture of detached 15 BL PEMs includes 2.5 BL of 5 % Gal-CS/HA/CS

Table 3.4 Assembly Conditions of Washed, Detachable and Free-standing 15 BL Gal-CS/HA/CS PEMs

Deposition Time (min)	Extent of galactosylation (%)	Number of layers with Gal-CS	pH of Gal-CS solution	pH of HA solution	pH of CS solution	pH of Water	Crosslinking Time with 8 w/v % GA (sec)	Detachability
50	5	5	4	4	5	4	-	Yes
50	5	5	4	4	5	4	20	Yes, but not robust
50	5	5	4	4	5	4	30	Yes, robust
50	5	5	4	4	5	4	40	Yes, robust
50	10	5	4	4	5	4	-	Yes
50	10	5	4	4	5	4	30	Yes, robust
50	-	-	-	4	5	4	30	Yes, robust

Chapter 4. Summary

4.1 Discussion and Conclusions

15 BL and 50 BL detachable and free-standing Gal-CS/HA/CS PEMs were prepared using the layer by layer method. The aim of the addition of galactose group to the PEMs was to promote the adhesion of hepatocytes.

50 BL free-standing detachable PEMs were fabricated and characterized at different cross-linking conditions. These PEMs contained either 5 BL or 10 BL of Gal-CS (5 % or 10 % galactosylation). They exhibited over 90 % weight retention after they were maintained at 37 °C for 7 days. According to the optical transmission data, PEMs have greater than 90 % transparency under hydrated conditions. PEMs have a smooth surface. The substrate side roughness of 4 % and 8 % GA cross-linked 5 % Gal-CS PEMs are 1.94 ± 2.51 nm and 2.25 ± 2.85 nm, respectively. The substrate side roughness of 4 % and 8 % GA cross-linked CS PEMs are 1.66 ± 2.15 nm and 2.3 ± 2.8 nm, respectively. The air side roughness of 4 % and 8 % GA cross-linked 5 % Gal-CS PEMs are 4.04 ± 5.03 nm and 4.3 ± 5.68, respectively.

4.2 Future Studies

In the future, PEMs containing Gal-CS can be used in hepatic tissue engineering applications. The cellular responses to the PEMs such as cytotoxicity and markers for hepatic functions can be investigated. In addition, the presence and localization of ASGP-R can be imaged using conventional immunostaining procedures. PEMs can be chemically modified with other ligands to promote adhesion with other hepatic cell types such as LSECs. The tri-peptide arginine-

glysine-aspartic acid (RGD) is a potential ligand for such an application since it can bind to integrins on LSECs.

4.3 References

1. Gero Decher, Y.L., Johannes Schmitt, *Proof of multilayer structural organization in self-assembled polycation-polyanion molecular films.* Thin Solid Films, 1994. **244**(1-2): p. 771-777.

2. Gero Decher, J.-D.H., *Buildup Of Ultrathin Multilayer Films By A Self-Assembly Process, 1 Consecutive Adsorption Of Anionic And Cationic Bipolar Amphiphiles On Charged Surfaces.* Makromol. Chem., Macromol. Symp, 1991. **46**(1): p. 321-327.

3. Vergaro, V., et al., *Drug-loaded polyelectrolyte microcapsules for sustained targeting of cancer cells.* Adv Drug Deliv Rev, 2011. **63**(9): p. 847-64.

4. Daubine, F., et al., *Nanostructured polyelectrolyte multilayer drug delivery systems for bone metastasis prevention.* Biomaterials, 2009. **30**(31): p. 6367-73.

5. Hajicharalambous, C.S., et al., *Nano- and sub-micron porous polyelectrolyte multilayer assemblies: biomimetic surfaces for human corneal epithelial cells.* Biomaterials, 2009. **30**(23-24): p. 4029-36.

6. Ren, K., et al., *Manipulation of the adhesive behaviour of skeletal muscle cells on soft and stiff polyelectrolyte multilayers.* Acta Biomater, 2010. **6**(11): p. 4238-48.

7. Fischlechner, M., et al., *Fusion of enveloped virus nanoparticles with polyelectrolyte-supported lipid membranes for the design of bio/nonbio interfaces.* Nano Lett, 2007. **7**(11): p. 3540-6.

8. Yoo, P.J., et al., *Solvent-assisted patterning of polyelectrolyte multilayers and selective deposition of virus assemblies.* Nano Lett, 2008. **8**(4): p. 1081-9.

9. Hiller, J., J.D. Mendelsohn, and M.F. Rubner, *Reversibly erasable nanoporous anti-reflection coatings from polyelectrolyte multilayers.* Nat Mater, 2002. **1**(1): p. 59-63.

10. Larkin, A.L., R.M. Davis, and P. Rajagopalan, *Biocompatible, detachable, and free-standing polyelectrolyte multilayer films.* Biomacromolecules, 2010. **11**(10): p. 2788-96.

11. Swierczewska, M., et al., *Cellular response to nanoscale elastin-like polypeptide polyelectrolyte multilayers.* Acta Biomater, 2008. **4**(4): p. 827-37.

12. Lingstrom, R. and L. Wagberg, *Polyelectrolyte multilayers on wood fibers: influence of molecular weight on layer properties and mechanical properties of papers from treated fibers.* J Colloid Interface Sci, 2008. **328**(2): p. 233-42.

13. Lingstrom, R., L. Wagberg, and P.T. Larsson, *Formation of polyelectrolyte multilayers on fibres: influence on wettability and fibre/fibre interaction.* J Colloid Interface Sci, 2006. **296**(2): p. 396-408.

14. Florin Bucatariu, G.F., Gabriela Hitruc, Ecaterina Stela Dragan, *Single polyelectrolyte multilayers deposited onto silica microparticles and silicon wafers.* Colloids and Surfaces A: Physicochem. Eng. Aspects, 2011. **380**(1-3): p. 111–118.

15. Olivier Félix, Z.Z., Fabrice Cousin, Gero Decher, *Are sprayed LbL-films stratified? A first assessment of the nanostructure of spray-assembled multilayers by neutron reflectometry.* C. R. Chimie, 2009. **12**(1-2): p. 225-234.

16. Hoogeveen, N.G., et al., *Formation and stability of multilayers of polyelectrolytes.* Langmuir, 1996. **12**(15): p. 3675-3681.

17. Decher, G., *Fuzzy Nanoassemblies: Toward Layered Polymeric Multicomposites.* Science, 1997. **277**(5330): p. 1232-1237

18. Davor Kovacevic , S.B., Josip Pozar, *The Influence of Ionic Strength, Electrolyte Type And Preparation Procedure on Formation of Weak Polyelectrolyte Complexes.* Colloids and Surfaces A: Physicochem. Eng. Aspects, 2007. **302**(1-3): p. 107–112.

19. Dubas, S.T. and J.B. Schlenoff, *Factors controlling the growth of polyelectrolyte multilayers.* Macromolecules, 1999. **32**(24): p. 8153-8160.

20. Thompson, M.T., et al., *Tuning compliance of nanoscale polyelectrolyte multilayers to modulate cell adhesion.* Biomaterials, 2005. **26**(34): p. 6836-45.

21. Kolasinska, M., R. Krastev, and P. Warszynski, *Characteristics of polyelectrolyte multilayers: effect of PEI anchoring layer and posttreatment after deposition.* J Colloid Interface Sci, 2007. **305**(1): p. 46-56.

22. Chua, P.H., et al., *Surface functionalization of titanium with hyaluronic acid/chitosan polyelectrolyte multilayers and RGD for promoting osteoblast functions and inhibiting bacterial adhesion.* Biomaterials, 2008. **29**(10): p. 1412-21.

23. Muthukumar, M., *Adsorption of a Polyelectrolyte Chain to a Charged Surface.* Journal of Chemical Physics, 1987. **86**(12): p. 7230-7235.

24. Wiegel, F.W., *Adsorption of a Macromolecule to a Charged Surface.* Journal of Physics a-Mathematical and General, 1977. **10**(2): p. 299-303.

25. Schlenoff, J.B. and S.T. Dubas, *Mechanism of polyelectrolyte multilayer growth: Charge overcompensation and distribution.* Macromolecules, 2001. **34**(3): p. 592-598.

26. Chung, A.J. and M.F. Rubner, *Methods of loading and releasing low molecular weight cationic molecules in weak polyelectrolyte multilayer films.* Langmuir, 2002. **18**(4): p. 1176-1183.

27. Dalgleish, D.G. and E.R. Morris, *Interactions between carrageenans and casein micelles: electrophoretic and hydrodynamic properties of the particles.* Food Hydrocolloids, 1988. **2**(4): p. 311-320.

28. Schoeler, B., et al., *Polyelectrolyte films based on polysaccharides of different conformations: Effects on multilayer structure and mechanical properties.* Biomacromolecules, 2006. **7**(6): p. 2065-2071.

29. Glinel, K., et al., *Influence of polyelectrolyte charge density on the formation of multilayers of strong polyelectrolytes at low ionic strength.* Langmuir, 2002. **18**(4): p. 1408-1412.

30. Ladam, G., et al., *In situ determination of the structural properties of initially deposited polyelectrolyte multilayers.* Langmuir, 2000. **16**(3): p. 1249-1255.

31. Caruso, F., et al., *Investigation of electrostatic interactions in polyelectrolyte multilayer films: Binding of anionic fluorescent probes to layers assembled onto colloids.* Macromolecules, 1999. **32**(7): p. 2317-2328.

32. Picart, C., et al., *Buildup mechanism for poly(L-lysine)/hyaluronic acid films onto a solid surface.* Langmuir, 2001. **17**(23): p. 7414-7424.

33. Picart, C., et al., *Molecular basis for the explanation of the exponential growth of polyelectrolyte multilayers.* Proc Natl Acad Sci U S A, 2002. **99**(20): p. 12531-12535.

34. Kujawa, P., et al., *Effect of molecular weight on the exponential growth and morphology of hyaluronan/chitosan multilayers: A surface plasmon resonance spectroscopy and atomic force microscopy investigation.* Journal of the American Chemical Society, 2005. **127**(25): p. 9224-9234.

35. Olson, J.A. and D. Gunning, *The storage form of vitamin A in rat liver cells.* J Nutr, 1983. **113**(11): p. 2184-91.

36. Powers, J.G. and B.A. Gilchrest, *What you and your patients need to know about vitamin d.* Semin Cutan Med Surg, 2012. **31**(1): p. 2-10.

37. Coleman, R., *Biochemistry of bile secretion.* Biochem J, 1987. **244**(2): p. 249-61.

38. Nemeth, E., A.W. Baird, and C. O'Farrelly, *Microanatomy of the liver immune system.* Semin Immunopathol, 2009. **31**(3): p. 333-43.

39. Remmer, H., *The role of theliver in drug metabolism.* Am J Med, 1970. **49**: p. 617-29.

40. Shibahara, S., T. Kitamuro, and K. Takahashi, *Heme degradation and human disease: diversity is the soul of life.* Antioxid Redox Signal, 2002. **4**(4): p. 593-602.

41. Jacobs, F., E. Wisse, and B. De Geest, *The role of liver sinusoidal cells in hepatocyte-directed gene transfer.* Am J Pathol, 2010. **176**(1): p. 14-21.

42. Lodish, H.F., N. Kong, and L. Wikstrom, *Calcium is required for folding of newly made subunits of the asialoglycoprotein receptor within the endoplasmic reticulum.* J Biol Chem, 1992. **267**(18): p. 12753-60.

43. Morell, A.G., et al., *Physical and chemical studies on ceruloplasmin. IV. Preparation of radioactive, sialic acid-free ceruloplasmin labeled with tritium on terminal D-galactose residues.* J Biol Chem, 1966. **241**(16): p. 3745-9.

44. Pricer, W.E., Jr. and G. Ashwell, *The binding of desialylated glycoproteins by plasma membranes of rat liver.* J Biol Chem, 1971. **246**(15): p. 4825-33.

45. Spiess, M., *The asialoglycoprotein receptor: a model for endocytic transport receptors.* Biochemistry, 1990. **29**(43): p. 10009-18.

46. Gregoriadis, G., et al., *Catabolism of desialylated ceruloplasmin in the liver.* J Biol Chem, 1970. **245**(21): p. 5833-7.

47. Weigel, P.H. and J.H. Yik, *Glycans as endocytosis signals: the cases of the asialoglycoprotein and hyaluronan/chondroitin sulfate receptors.* Biochim Biophys Acta, 2002. **1572**(2-3): p. 341-63.

48. Mizuno, M., W.R. Brown, and J.M. Vierling, *Ultrastructural immunocytochemical localization of the asialoglycoprotein receptor in rat hepatocytes.* Gastroenterology, 1984. **87**(4): p. 763-9.

49. Pricer, W.E., Jr. and G. Ashwell, *Subcellular distribution of a mammalian hepatic binding protein specific for asialoglycoproteins.* J Biol Chem, 1976. **251**(23): p. 7539-44.

50. Steer, C.J. and G. Ashwell, *Studies on a mammalian hepatic binding protein specific for asialoglycoproteins. Evidence for receptor recycling in isolated rat hepatocytes.* J Biol Chem, 1980. **255**(7): p. 3008-13.

51. Weigel, P.H. and J.A. Oka, *The large intracellular pool of asialoglycoprotein receptors functions during the endocytosis of asialoglycoproteins by isolated rat hepatocytes.* J Biol Chem, 1983. **258**(8): p. 5095-102.

52. Saranya, N., et al., *Chitosan and its derivatives for gene delivery.* Int J Biol Macromol, 2011. **48**(2): p. 234-8.

53. Liu, D., et al., *Determination of the degree of acetylation of chitosan by UV spectrophotometry using dual standards.* Carbohydr Res, 2006. **341**(6): p. 782-5.

54. Senel, S. and S.J. McClure, *Potential applications of chitosan in veterinary medicine.* Adv Drug Deliv Rev, 2004. **56**(10): p. 1467-80.

55. Muzzarelli, R.A.A., *Chitins and chitosans for the repair of wounded skin, nerve, cartilage and bone.* Carbohydrate Polymers, 2009. **76**(2): p. 167–182.

56. C. Qin, H.L., Q. Xiao, Y. Liu, J. Zhu, Y. Du, *Water-solubility of chitosan and its antimicrobial activity.* Carbohydrate Polymers, 2006. **63**(3): p. 367–374.

57. I.A. Sogias, V.V.K., A.C. William, *Exploring the Factors Affecting the Solubility of Chitosan in Water.* Macromolecular Chemistry and Physics, 2010. **221**(4): p. 426–433,.

58. Boudou, T., et al., *Polyelectrolyte multilayer nanoshells with hydrophobic nanodomains for delivery of Paclitaxel.* J Control Release, 2012.

59. Zivanovic, S., et al., *Physical, mechanical, and antibacterial properties of chitosan/PEO blend films.* Biomacromolecules, 2007. **8**(5): p. 1505-10.

60. Manna, U., S. Bharani, and S. Patil, *Layer-by-layer self-assembly of modified hyaluronic acid/chitosan based on hydrogen bonding.* Biomacromolecules, 2009. **10**(9): p. 2632-9.

61. Bhatnagar, A. and M. Sillanpaa, *Applications of chitin- and chitosan-derivatives for the detoxification of water and wastewater--a short review.* Adv Colloid Interface Sci, 2009. **152**(1-2): p. 26-38.

62. P. A. Sandford, A.S., *Biomedical Applications of High-Purity Chitosan Physical, Chemical, and Bioactive Properties.* ACS Symposium Series, 1991. **4467**: p. 430-445.

63. Kumar, R., *A review of chitin and chitosan applications.* Reactive & Functional Polymers, 2000. **46**(1): p. 1–27.

64. Kim, Y. and P. Rajagopalan, *3D hepatic cultures simultaneously maintain primary hepatocyte and liver sinusoidal endothelial cell phenotypes.* PLoS One, 2010. **5**(11): p. e15456.

65. Kim, Y., et al., *The design of in vitro liver sinusoid mimics using chitosan-hyaluronic acid polyelectrolyte multilayers.* Tissue Eng Part A, 2010. **16**(9): p. 2731-41.

66. Johansson, J.A., et al., *Build-up of collagen and hyaluronic acid polyelectrolyte multilayers.* Biomacromolecules, 2005. **6**(3): p. 1353-9.

67. Kogan, G., et al., *Hyaluronic acid: a natural biopolymer with a broad range of biomedical and industrial applications.* Biotechnol Lett, 2007. **29**(1): p. 17-25.

68. Xu, X., et al., *Hyaluronic Acid-Based Hydrogels: from a Natural Polysaccharide to Complex Networks.* Soft Matter, 2012. **8**(12): p. 3280-3294.

69. Lu, H. and N. Hu, *Loading behavior of {chitosan/hyaluronic acid}n layer-by-layer assembly films toward myoglobin: an electrochemical study.* J Phys Chem B, 2006. **110**(47): p. 23710-8.

70. L. Grossin, D.C., B. Saulnier, O. Felix, A. Chassepot, G. Decher, P. Netter, P. Schaaf, P. Gillet, D. Mainard, J. Voegel, N. Jessel, *Step-by-Step Build-Up of Biologically Active Cell-Containing Stratified Films Aimed at Tissue Engineering.* Adv. Mater., 2009. **21**(6): p. 650–655.

71. Rouse, J.J., et al., *Controlled drug delivery to the lung: Influence of hyaluronic acid solution conformation on its adsorption to hydrophobic drug particles.* Int J Pharm, 2007. **330**(1-2): p. 175-82.

72. A.H. Dent, M.A., *The Preparation of Protein-Protein Conjugates*, in *Bioconjugation*1998, Grove's Dictionaries INC: New York. p. 228.

73. Chung, T.W., et al., *Preparation of alginate/galactosylated chitosan scaffold for hepatocyte attachment.* Biomaterials, 2002. **23**(14): p. 2827-34.

74. Chu, X.H., et al., *In vitro evaluation of a multi-layer radial-flow bioreactor based on galactosylated chitosan nanofiber scaffolds.* Biomaterials, 2009. **30**(27): p. 4533-8.

75. Seo, S.J., et al., *Alginate/galactosylated chitosan/heparin scaffold as a new synthetic extracellular matrix for hepatocytes.* Tissue Eng, 2006. **12**(1): p. 33-44.

76. A. Hirai, H.O., A. Nakajima, *Determination of degree of deacetylation of chitosan by ^{1}H NMR spectroscopy.* Polymer Bulletin, 19991. **26**(1): p. 87-94.

77. Park, I.K., et al., *Galactosylated chitosan as a synthetic extracellular matrix for hepatocytes attachment.* Biomaterials, 2003. **24**(13): p. 2331-7.

78. Kim, T.H., et al., *Galactosylated chitosan/DNA nanoparticles prepared using water-soluble chitosan as a gene carrier.* Biomaterials, 2004. **25**(17): p. 3783-92.

79. Chung, T.W., et al., *Preparation of alginate/galactosylated chitosan scaffold for hepatocyte attachment.* Biomaterials, 2002. **23**(14): p. 2827-2834.

80. Park, I.K., et al., *Galactosylated chitosan as a synthetic extracellular matrix for hepatocytes attachment.* Biomaterials, 2003. **24**(13): p. 2331-2337.

81. Kim, E.M., et al., *Hepatocyte-targeted nuclear imaging using Tc-99m-galactosylated chitosan: Conjugation, targeting, and biodistribution.* Journal of Nuclear Medicine, 2005. **46**(1): p. 141-145.

82. Almodovar, J., et al., *Layer-by-layer assembly of polysaccharide-based polyelectrolyte multilayers: a spectroscopic study of hydrophilicity, composition, and ion pairing.* Biomacromolecules, 2011. **12**(7): p. 2755-65.

83. Boudou, T., et al., *Internal composition versus the mechanical properties of polyelectrolyte multilayer films: the influence of chemical cross-linking.* Langmuir, 2009. **25**(24): p. 13809-19.

84. Brown, M.B. and S.A. Jones, *Hyaluronic acid: a unique topical vehicle for the localized delivery of drugs to the skin.* Journal of the European Academy of Dermatology and Venereology, 2005. **19**(3): p. 308-318.

85. Domard, A., *Ph and Cd Measurements on a Fully Deacetylated Chitosan - Application to Cu-Ii-Polymer Interactions.* Int J Biol Macromol, 1987. **9**(2): p. 98-104.

86. Leung, H.W., *Ecotoxicology of glutaraldehyde: review of environmental fate and effects studies.* Ecotoxicol Environ Saf, 2001. **49**(1): p. 26-39.